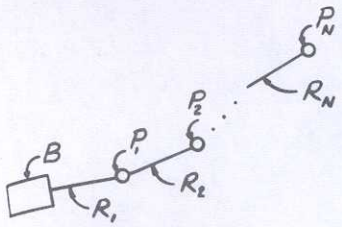

Fig. 3. Proposed example.

numerical integration, the former set of equations is considerably more convenient than is the latter. Indeed, to bring Eqs. (41)–(43) into a computer-integrable form, one must first eliminate λ_1, a task that has no counterpart in connection with the formulation of dynamical equations based on Eq. (1). Moreover, once this elimination has been accomplished, one is still faced with equations coupled in the highest derivatives of dependent variables. The earlier equations are free of such coupling.

The differences between using Eqs. (1) and Eqs. (37) become ever greater as the systems to be analyzed become ever more complex. The reader may find it interesting to test this proposition by formulating equations of motion for the system shown in Fig. 3, assuming that P_i is unable to move perpendicularly to R_i $(i = 1,...,N)$.

VI. CONCLUSION

As is well known, one of the most important attributes of Lagrange's equations of motion is that their use permits the automatic elimination of certain internal and external constraint forces, namely, those associated with workless, holonomic constraints. Constraint forces associated with workless, nonholonomic constraints come into evidence via Lagrange multipliers and must be eliminated by algebraic means. In order to be able to employ the Lagrange equations, one must work with generalized coordinates, which both can increase the labor one must perform to generate dynamical differential equations and can lead to unnecessarily complex equations. By way of contrast, the use of Eqs. (1) permits the automatic elimination of *all* constraint forces associated with workless constraints, and it leads to equations having the simplest possible form, provided generalized speeds are selected optimally.

[1]T. R. Kane, P. W. Likins, and D. A. Levinson, *Spacecraft Dynamics* (McGraw–Hill, New York, 1983), p. 248.
[2]Reference 1, p. 259.
[3]H. Goldstein, *Classical Mechanics*, 2nd ed. (Addison-Wesley, Reading, MA, 1980), p. 47.
[4]T. R. Kane and D. A. Levinson, AIAA J. **3** (2), 99 (1980).

Solitons in undergraduate laboratory

Alessandro Bettini, Tullio A. Minelli, and Donatella Pascoli
Istituto di Fisica "G. Galilei," Università di Padova, Via Marzolo, 8-35100 Padova, Italy

(Received 6 October 1982; accepted for publication 2 February 1983)

Teaching nonlinear phenomena, from an experimental point of view, in a laboratory for undergraduates in physics has been a motivating experience. We report in this paper on an advanced undergraduate laboratory on solitons in water. After recalling the main aspects of the theory and the principal characteristics of the solitons, the experimental apparatus is described and the results obtained by some students are discussed. A systematic check of the properties of solitons is obtained. An overall evaluation of the laboratory is given at the end.

I. INTRODUCTION

The study of wave phenomena in physics has been practically limited until recent years to linear systems; the situation dramatically changed after the discovery of the solitons,[1] localized nonlinear waves that maintain their identity even after a collision. Triggered by this discovery many nonlinear dispersive systems have been theoretically described in terms of partial differential equations that admit soliton solutions. In particular, on the free surface of the water, solitary waves can develop and propagate as observed, historically for the first time in 1834, by John Scott Russell in his celebrated "Report on waves."[2]

The purpose of this paper is to report on a basic laboratory to study the principal characteristics of solitons in water that we have developed for majors in Physics at the University of Padova.

After recalling the main aspects of the theory in Sec. II, we will describe the experimental apparatus in Sec. III, and present some of the results obtained by our students in Sec. IV. An overall evaluation of the laboratory and a brief conclusion will close the article.

II. THE SOLITONS

We start by recalling briefly the important historical facts. After the above-mentioned observation of solitary waves by Scott Russell, Korteveg and de Vries[3] developed, at the end of the last century, a theoretical description of the solitary waves in terms of a nonlinear partial differential equation (KdV equation). The next important step forward was made 70 years later by Zabusky and Kruskal,[1] who simulated in a computer experiment the collision of two solitary waves described by the KdV equation. It had

been generally believed till then that two colliding solitary waves would interact so strongly (and nonlinearly) as to destroy each other. The surprising results of Zabusky and Kruskal were that the waves re-emerge after the collision with unvaried shapes and speeds. This similarity with the behavior of particles is at the origin of the name "soliton." In summary, a solitary wave is a wave that travels with unaltered shape, a soliton is a solitary wave whose shape and speed are not altered by a collision.

We will now recall briefly the theory of Korteweg and de Vries; detailed derivation may be found elsewhere.[4] Assume that the liquid is homogeneous, incompressible, and with zero viscosity. Note that the last assumption is far from being true for any real liquid. Let us assume further that the liquid is contained in a channel along the x axis with a horizontal bed at the constant depth $z = -h$ and with a constant width $\Delta y = w$. The liquid is subject to the vertical gravitational force (g) and to the constant atmospheric pressure acting on its free surface. We will forget surface tension effects; as we will see, this is reasonable with our working depths. Finally, the motion of the liquid under the action of these forces is assumed to be irrotational.

In the above assumptions we are considering one-dimensional waves propagating along the channel. We will denote with $\eta(x,t)$ the vertical displacement at the same time t of the liquid particle at the free surface that is at x when in equilibrium.

The above assumptions do not suffice to specify the shape and the behavior of the waves. To define the solutions we must make assumptions of the relative values of three characteristic lengths: the vertical displacement η (the amplitude of the wave), a typical horizontal dimension l of the wave (for example the wavelength for a sinusoidal wave train), and the depth of the channel h.

If $\eta/l \ll 1$, the classical dispersive linear case ("infinitesimal" waves), we obtain the well-known dispersion relation:

$$\omega^2 = kg + \tanh(kh), \tag{1}$$

where k is the wavenumber and ω the (angular) frequency.

In this work we will be always concerned with shallow water waves. In this case kh (or h/l) is small. The dispersion relation (1) can then be written:

$$\omega = c_0[k - (h^2/6)k^3 + \ldots], \tag{2}$$

where

$$c_0 = (gh)^{1/2}. \tag{3}$$

If the depth h is very small, the development can be stopped at the first term in kh and we are left with the well-known nondispersive shallow water waves of speed c_0. As the value of kh increases and the term in k^3 must be included, the waves become dispersive and we have one of the terms of the KdV equation.[5] The second important term, that gives the nonlinearity, comes in when terms in η/h are included. This gives a correction to the speed that becomes an increasing function of the amplitude, given by

$$c = c_0(1 + 3\eta/2h). \tag{4}$$

In synthesis, the KdV equation is obtained under the following assumptions:

(i) Small-amplitude waves. If $\bar{\eta}$ represents a typical wave amplitude:

$$\epsilon_1 \equiv \bar{\eta}/h \ll 1. \tag{5i}$$

(ii) Long waves. If l is a typical horizontal wave dimension:

$$\epsilon_2 \equiv (h/l)^2 \ll 1. \tag{5ii}$$

(iii) The two effects approximately balance; i.e., ϵ_1 and ϵ_2 have the same order of magnitude. By defining the "Ursell number"

$$U \equiv \epsilon_1/\epsilon_2 = \bar{\eta} l^2/h^3, \tag{6}$$

we require that

$$U = O(1), \tag{5iii}$$

where $O(1)$ means of the order of unity.

The KdV equation, obtained under the above assumptions, is

$$\eta_t + c_0\eta_x + (3c_0/2h)\eta\eta_x + (c_0h^2/6)\eta_{xxx} = 0, \tag{7}$$

where the subscripts refer to derivatives with respect to t and x. The equation describes waves advancing in the positive x direction; a similar but separate equation describes waves moving in the negative x direction.

A qualitative justification of Eq. (7) can be obtained identifying the nonlinear term $c_0(3\eta/2h)\eta_x$ with the term appearing in (4) and the dispersive term $(c_0h^2/6)\eta_{xxx}$ with that of Eq. (2). The rigorous justification is obtained through a development in the two above defined parameters ϵ_1 and ϵ_2.

The solitary wave solutions of Eq. (7) emerge due to the competition between the nonlinear and the dispersive terms. Under certain conditions the two exactly balance, the result being a stable configuration, a wave that moves without any change of shape (as those caused by each one of the two terms separately). The solitary wave solution of the KdV equation specifies analytically the shape of the wave:

$$\eta(x,t) = \eta_0 \operatorname{sech}^2[(x - ct)/L], \tag{8}$$

where η_0 is the maximum amplitude of the wave, c its speed, given for the wave (8) by

$$c = c_0(1 + \eta_0/2h), \tag{9}$$

and

$$L = (4h^3/3\eta_0)^{1/2} \tag{10}$$

the characteristic length of the wave. The solitary wave is a single bell-shaped wave as shown in Fig. 1, very different from the normal sine-like trains of waves of the linear case.

A further important contribution to the development of the theory was given in 1967 by Gardner *et al.*[6] who showed that, if the initial shape of the wave is "sufficiently localized," the analytical solution of the KdV equation can be obtained. The solution predicts that, if the total initial

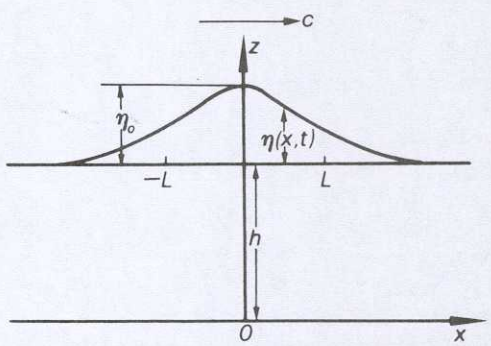

Fig. 1. A solitary wave advancing in the positive x direction at the speed c. Speed c, height η_0, and length $\mathscr{L}$ are correlated. The vertical scale is expanded with respect to the horizontal by a factor of the order of 100.

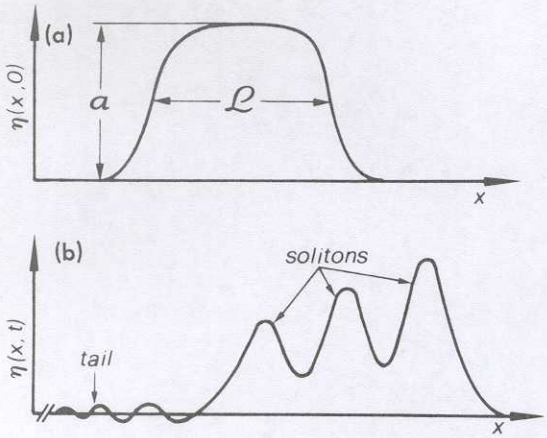

Fig. 2. Evolution of an initially confined disturbance in a set of solitons followed by a radiative tail.

volume is non-negative, the wave evolves in one or more solitons and a dispersive "radiative tail" at sufficiently long times, as sketched in Fig. 2. These results are obtained through the so-called inverse scattering method where the problem is reduced to find the eigenstates of the Schrödinger equation with a "potential well" having the shape of the initial wave inverted in sign. A one-to-one correspondence exists between the bound states and the solitons asymptotically evolving from the initial wave, and between the scattering states and the radiative tail.

The total number N of solitons depends on the initial shape and on the depth of the liquid h. We will limit our experiments to rectangular initial waves (advancing in x direction) of length $\mathscr{L}$ and height a. In this case

$$N = 1 + \mathrm{Int}(S/\pi), \quad S = (3a/2h)^{1/2}\,\mathscr{L}/h\,, \tag{11}$$

where Int means "integer part of."

The essential results of the theory of solitons described by the KdV equation may be summarized in the following list of main predictions that we will check in our experiments:

(1) From an initial disturbance of non-negative volume which is sufficiently localized at least one solitary wave evolves, whose shape is given by (8), that in particular links wave amplitude, length, and velocity.

(2) The shape of each solitary wave does not vary, after the stable state is reached.

(3) The number of solitary waves evolving from an initial rectangular wave is given by (11).

(4) The solitary waves are followed by a dispersive tail.

(5) The speed of the solitary waves depends linearly on their amplitude as predicted by (9).

(6) Since the larger solitary waves travel faster, they evolve in groups which are rank-ordered.

(7) The solitary waves are stable under collisions when traveling in the same direction, hence they are solitons. A collision can be obtained by launching a smaller soliton followed by a larger one. This last soliton will travel faster and ultimately reach and overtake the smaller soliton. The KdV predicts that the shapes after the interaction remain unaltered; the solitons experience only a phase shift, advancing the faster and retarding the slower. More precisely, in the case of two interacting solitons of amplitudes η_{01} and η_{02} ($\eta_{01} > \eta_{02}$), the time shifts are given by[7]

$$\begin{aligned} \Delta_1 &= (h/c_1)(1/K_1)\ln[(K_1+K_2)/(K_1-K_2)] \\ \Delta_2 &= (h/c_2)(1/K_2)\ln[(K_1+K_2)/(K_1-K_2)]\,, \end{aligned} \tag{12}$$

where

$$K_i = (3\eta_{0i}/4h)^{1/2}$$

and c_i are the speeds of each soliton according to (9).

(8) The solitons are also stable under head-on collisions. This is not a prediction of the KdV equation: The two colliding waves travel, in fact, in opposite directions and are described by two separate KdV equations. Nonetheless this is believed to be a characterizing property of solitons.

III. EXPERIMENTAL APPARATUS

To develop the experimental program defined in the previous section we must be able to produce an initial rectangular disturbance on the free surface of the water contained in a channel, sufficiently long to allow the evolution of the initial state into one or more solitons and then to observe their propagation and their collisions. Experiments of this type were performed in a big wave tank by Hammack and Segur.[8] In our case the dimensions must be such as to allow the accommodation of the tank in the students' laboratory.

The critical dimension of the tank is obviously its length, that is defined by the distance that two or more solitons must travel to separate from each other, due to the dependence of the speed on the amplitude (9). The relative difference in speed between two solitons of amplitude η_1 and η_2 is essentially $(c_1 - c_2)/c_0 = (\eta_1 - \eta_2)/2h$. If we define the "separation distance" D_{sep} as the distance after which the two solitons are separated by a characteristic length L (10), we can take

$$D_{\mathrm{sep}} = (4h^2/\Delta\eta)\,(h/3\eta_0)^{1/2}\,, \tag{13}$$

where $\Delta\eta = |\eta_1 - \eta_2|$ and η_0 is the average of η_1 and η_2. Note that relatively high waves (bigger values of η_0 and $\Delta\eta$) are characterized by smaller values of D_{sep}. For example, with $\eta_0 \simeq 1$ cm, $\Delta\eta \simeq 0.3$ cm, and a water depth $h \simeq 5$ cm, $D_{\mathrm{sep}} \simeq 4$ m.

To allow easy observations on fully separated solitons and to study their collisions we built a tank 12 m long; its depth is 15 cm, its width 8 cm. The tank consists in eight elements each 1.5 m long made from polished perspex; flanges with O-rings provide the connections of consecutive elements. Screws on each element provide the necessary horizontal alignment. At the end of the tank opposite to that where waves are produced, a smoothly degrading pebble beach (partially) absorbs the incoming waves, limiting annoying reflections.

We detect the solitons by recording the variations in depth (function of time) by measuring the variation of the electric resistance between two electrodes immersed in the water. The depth variation is of the order of a few millimeters.

The resistance between two identical cylindrical conductors dipped at a depth z in a fluid of conductance σ is given by

$$R(z) = (1/\pi\sigma z)\ln(2l/D)\,, \tag{14}$$

where l is the length and D the diameter of the conductors ($D \ll l$). If z_0 is the static draught of the electrodes, and Δz its variation, the corresponding specific variation of the resistance is

$$\Delta R/R = -(\Delta z/z_0)/(1 + \Delta z/z_0)\,. \tag{15}$$

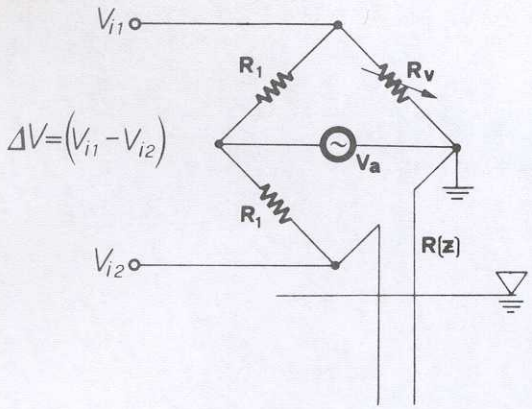

Fig. 3. Bridge circuit to measure the level of the water.

The bridge shown in Fig. 3 (in ac to avoid electrode polarization) gives the signal

$$\Delta V = V_a \left(\frac{\Delta z/z_0}{\alpha(\beta + \Delta z/z_0)} \right),$$

with

$$\alpha = 1 + \frac{R_1}{R_v}, \quad \beta = 1 + \frac{R_v}{R_1}. \tag{16}$$

The variable resistor R_v is used to balance the bridge for each value of the static depth z_0. The relation (16) can be assumed to be linear if $\Delta z/z_0 \ll \beta$.

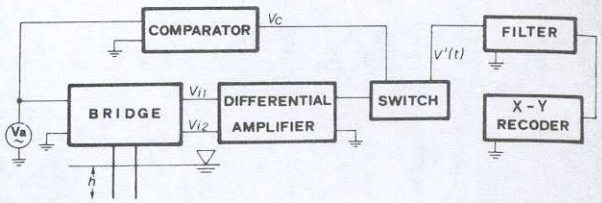

Fig. 4. Block diagram of the electronics.

The signal from the bridge must be amplified and rectified. The block diagram is shown in Fig. 4. If the polarization voltage is $V_a(t) = V_a \sin \omega t$, the signal, amplified by a differential amplifier of gain A, is

$$V(t) = (V_a A / z_0 \alpha\beta)\Delta z(t) \sin \omega t .$$

Note that $V(t)$ is in phase with the carrier for positive values of Δz. To reconstruct the original waveform we recognize the phase of $V(t)$ relative to the carrier via a switch controlled by a square wave obtained, via a comparator, from the carrier. After the switch the signal is

$$V'(t) = \begin{cases} (AV_a/z_0\alpha\beta)\Delta z(t) \sin \omega t , & \text{for } \sin \omega t > 0 \\ 0 , & \text{for } \sin \omega t < 0 . \end{cases}$$

Finally the carrier ($\omega/2\pi = 10$ kHz) is suppressed by a

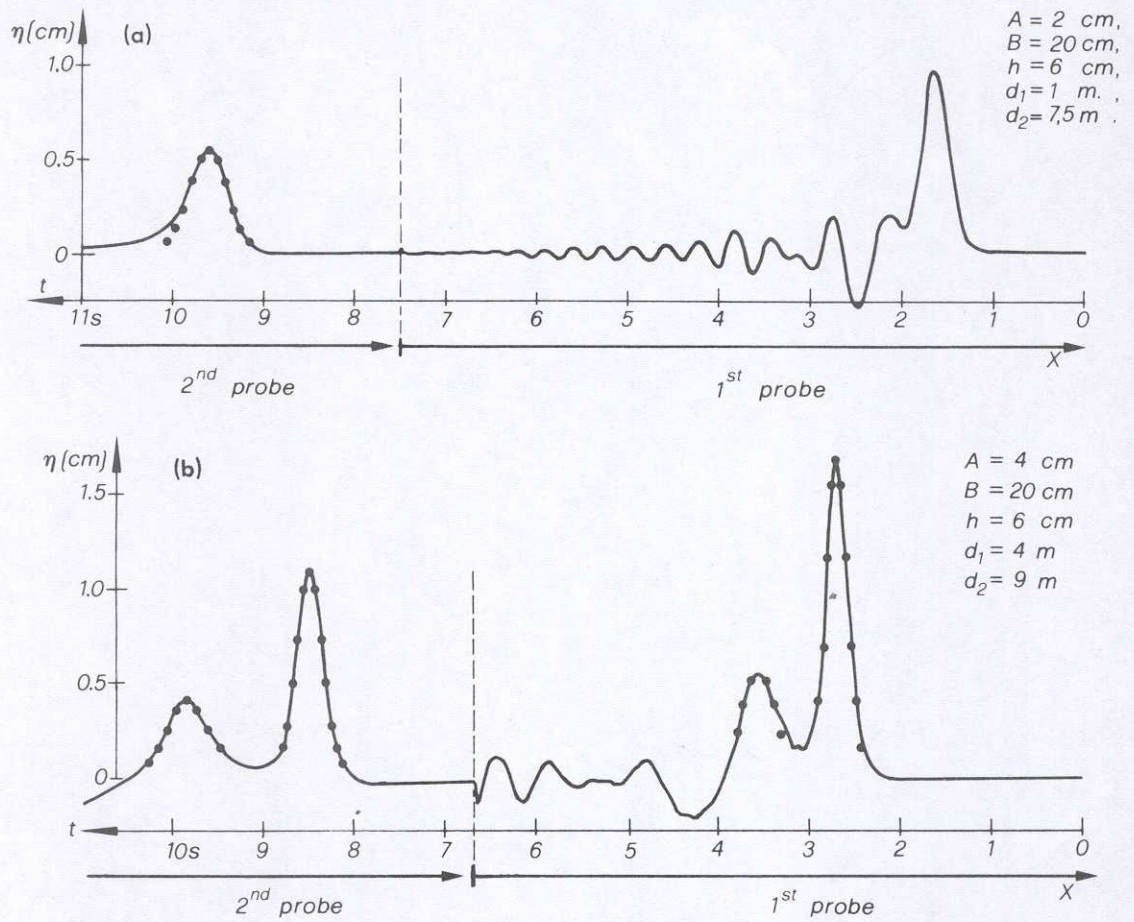

Fig. 5. (a) Record of the water level at the two probes located at $d_1 = 1$ m, $d_2 = 7.5$ m from the beginning of the tank. The wave was originated by preparing an initial step of height $A = 4$ cm and length $B = 20$ cm in water of depth $h = 6$ cm. Dots are calculated from (8) with η_0 adjusted at the soliton top. (b) Similar record in the conditions shown in the insert.

Table I. Comparison of the number of observed and predicted solitons.

A (cm)	B (cm)	h (cm)	N_{obs}	N_{pred}	$U = \mathscr{L}^2 a/h^3$	
2	20	6	1	2	7.4	[Fig. 5(a)]
3	20	6	2	2	11.2	
4	20	6	2	2	14.8	[Fig. 5(b)]
1	40	6	2	2	7.6	
2	40	6	3	3	15.4	
3	40	6	3	3	23.	
3	20	3	3	4	88.	
3	10	4	2	2	9.4	
3	20	4	3	3	37.6	
2	20	4	2	2	25	
3	30	4	4	4	84.4	
2	30	4	3	3	56.2	
3	40	4	5–6	5	150	
2	40	4	4	4	100	

two-stage active filter and the signal (at frequencies of the order of the Hertz) sent to an xy recorder.

In the experiments we will describe, two probes at different positions along the tank were used. As only one xy recorder was available, each of the electronic channels associated with the two probes could be connected to the recorder via a manual switch that was commuted from the first to the second probe during the transit time of the wave between them. The examples of Fig. 5 show both signals on the same time scale.

Note that we detect the variation of the depth as a function of the time; this can be interpreted as the wave profile if, as is practically true in our case, the wave shape does not vary appreciably during the observation. The wave shape appears of course in our records with respect to an x axis running opposite to the time axis.

A simple way to produce an initial rectangular disturbance consists in closing an initial segment of the length B of the tank by a "weir" (made from perspex with a rubber lining on the border) up to a height A over the free level. A handle allows rapid extraction of the weir. As noted by Hammack and Segur,[8] the nearest closed end of the tank acts as a reflection plane for the wave, that immediately after the extraction is approximately rectangular[9] with length $\mathscr{L} = 2B$ and height $a = A/2$. This must be taken into account when computing the expected number of solitons.

IV. EXPERIMENTAL RESULTS

We will report here the results obtained by a group of students[10] that also were asked to design, build, test, and calibrate the electronics. We go directly to check the eight predictions of Sec. II.

(1) Figure 5(a) shows a record (see figure captions for the initial conditions) where one soliton appears. At the first probe it is still interacting with the tail, while at the second it is almost free from it. The dots show the shape expected from formula (8) with η_0 normalized to the maximum amplitude of the wave. The agreement is rather good. Figure 5(b) shows two solitons; again comparison with formula (8) shows good agreement.

(2) The invariance of the shape predicted by the theory cannot of course be exactly verified due to the presence of dissipative forces that reduce the amplitude of the wave during its propagation, as is clearly seen in Fig. 5. What is conserved is the shape, normalized to the decreasing amplitude η_0 as shown in Fig. 5(b).

(3) Equation (11) gives the number of solitons evolving from an initial rectangular wave. To test this prediction waves were produced with different values of height A and length B of the static initial state and of the depth h of the tank. The relevant parameters and the predicted N_{pred} and observed N_{obs} numbers of solitons are reported in Table I. Recalling assumptions (5i)–(5iii), note that assumption (5iii)

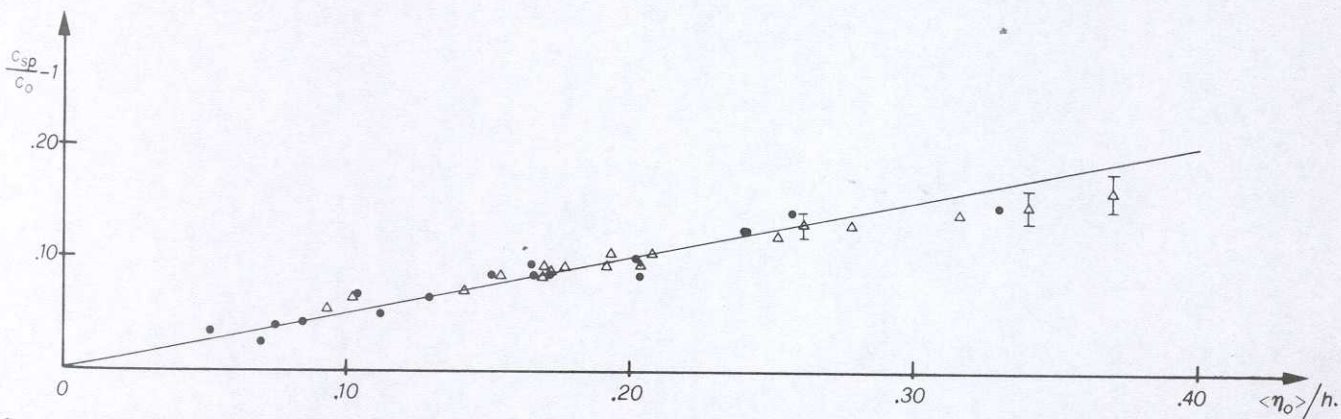

Fig. 6. Relative difference of the measured speed c_{sp} from c_0 versus relative average amplitude $\langle \eta_0 \rangle / h$ for a sample of 35 solitons. The line is the prediction of formula (9). (● Data for $h = 6$ cm, Δ for $h = 4$ cm.)

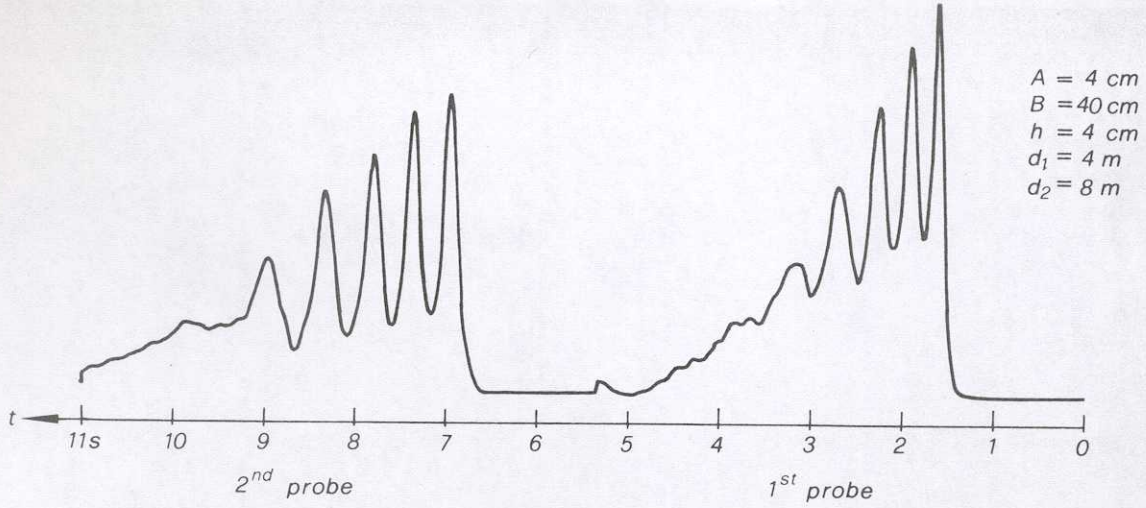

Fig. 7. Record showing five rank-ordered solitons advancing at different speeds.

is not in fact well specified: the "typical horizontal wave dimensions l" is not in fact exactly defined. To compute U we have taken the length $l = \mathscr{L} = 2B$ and the height $a = A/2$ of the initial disturbance. Looking now at Table I we see a discrepancy in the first row. This is not serious, the prediction being marginal: $N_{\text{pred}} = \text{Int}(2.06)$. In the seventh row we have the only real discrepancy; it happens for high values both of $a/h = 0.5$ and $U = 88$; moreover, the water depth h is only 3 cm and surface tension effects are expected to be more important. We are probably outside the range of validity of the KdV equation (this is probably true also for the last two rows where the predictions are satisfied).

(4) The radiative tail can be observed in Fig. 5(a) (in other cases it has been "cut out" from the graph). The tail is dispersive, the longer wavelengths leading the shorter.

(5) To study the dependence of the speed from the amplitude 19 records were taken with different initial conditions; excluding the solitons that were still interacting at the first probe, we were left with a sample of 35 solitons of which we determined the speed, c_{sp}, simply as the ratio of the distance between the probes, $d = 5$ m, and the time taken to travel that distance. On this long base the amplitude of each soliton falls appreciably due to the viscosity. To compare our data with theory we have then plotted in Fig. 6 the quantity $c_{sp}/\sqrt{gh} - 1$ vs $\langle \eta_0 \rangle / h$, were $\langle \eta_0 \rangle$ is the average of the amplitudes as measured at the two probes. The expected linear behavior is observed in agreement with the theory inside the experimental errors that are of the same order of the scatter of the points.

(6) Since, as we have just seen, the larger solitons travel faster, they form groups, which are rank-ordered with the larger leading the smaller. An example is given in Fig. 7. Note that the peaks of the solitons lay approximately on a straight line. This is due to the fact that relative velocities of the solitons and hence the distances covered are proportional to their amplitude.

(7) To study the overtaking between solitons a smaller soliton followed by a higher one must be launched. This was done as shown schematically in Fig. 8(a). With $B_1 = B_2 = 20$ cm, $A_1 = 2$ cm, $A_2 = 4$ cm, and $h = 6$ cm the record shown in Fig. 9(a) at the two probes at $d_1 = 1.9$ m, $d_2 = 8.9$ m was obtained. It is evident that the highest soliton overtook one of the smaller between the probes. The behavior of each of the two waves, when alone (i.e., noninteracting) was recorded preparing the waves as sketched in Fig. 8(b) and (c), respectively. The curves are reported in Fig. 9(b) and (c). The invariance of the shape is qualitatively observed. We also observe the phase shifts that advance the faster and retard the slower. From the figure we compute a phase shift $\Delta_1 = (0.35 \pm 0.02)$ s for the soliton amplitude $\eta_{01} = (12 \pm 1)$ mm and $\Delta_2 = -(0.45 \pm 0.02)$ s for the soliton amplitude $\eta_{02} = (6 \pm 0.5)$ mm. These results are in agreement with the theoretical predictions as given by (12): $\Delta_1 = (0.31 \pm 0.03)$ s, $\Delta_2 = (-0.47 \pm 0.05)$ s.

(8) To study the stability of the solitons in head-on collisions, two rectangular initial waves were generated at the same time at the two ends of the tank. One of the two evolving groups of solitons is observed before the collision at the first probe and after the collision at the second. One example is given in Fig. 10 (continuous curve). The observed

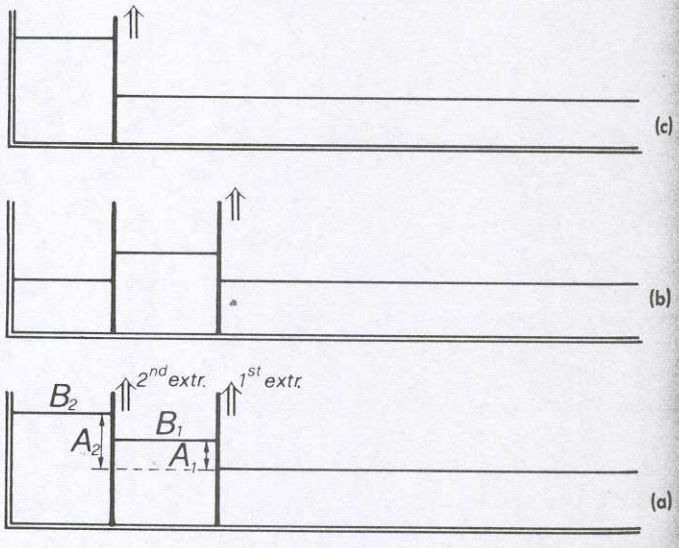

Fig. 8. Shows schematically the procedure used for recording the overtaking between solitons.

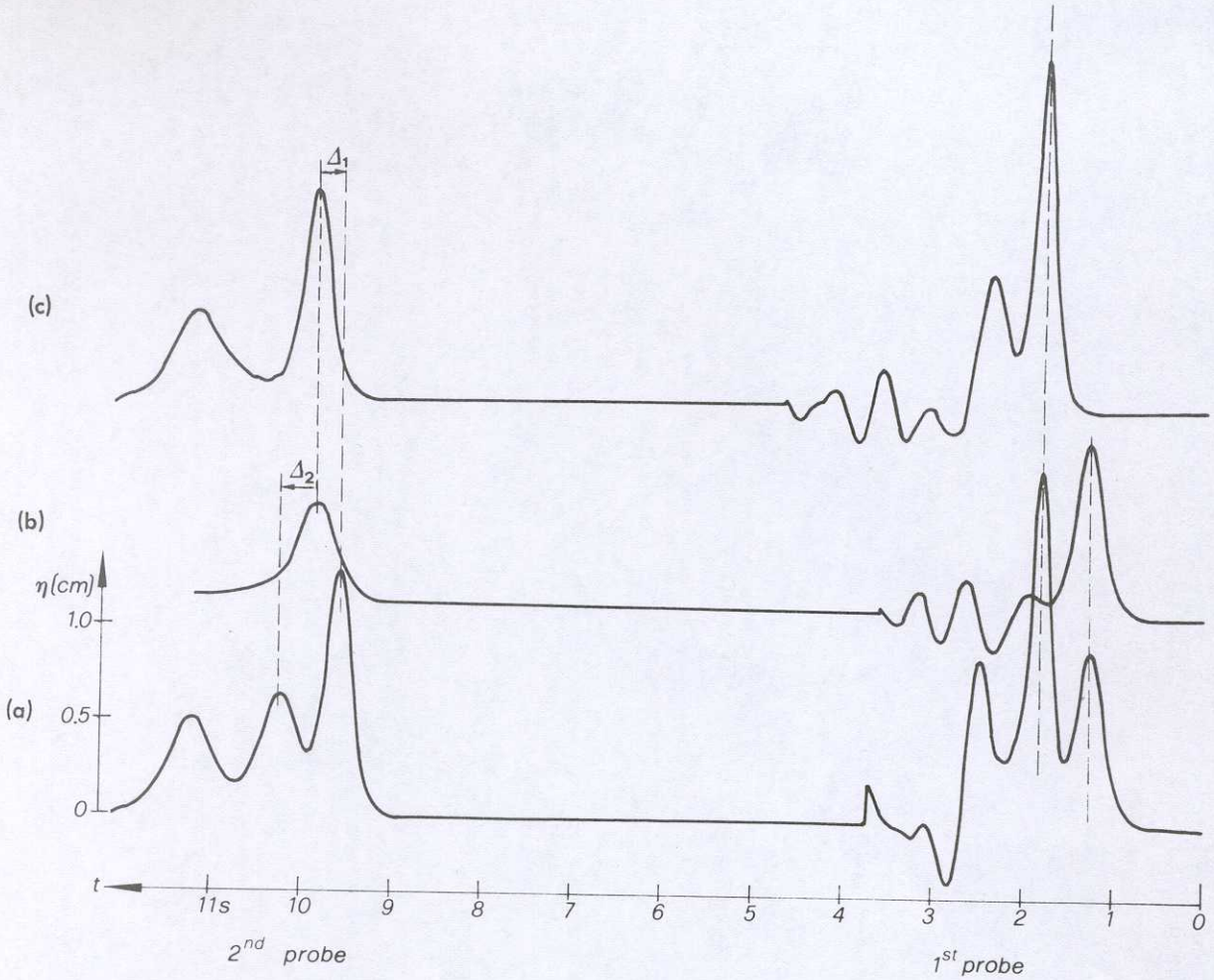

Fig. 9. Record obtained with the procedure sketched in Fig. 8, with $A_1 = 2$ cm, $A_2 = 4$ cm, $B_1 = B_2 = 20$ cm, and $h = 6$ cm at two probes at $d_1 = 1.9$ m, $d_2 = 8.9$ m. With the procedure of Figs. 8(a) the record in Fig. 9(a) is obtained. The biggest soliton advanced the smaller between the probes. Record 9(b) obtained as shown in Fig. 8(b) shows the overtaking wave when alone. Record 9(c) obtained as shown in Fig. 8(c) shows the evolution of the overtaken soliton when alone (without interaction). The time scale origins of the records have been properly adjusted as shown to allow direct observation of the phase shifts Δ_1 and Δ_2.

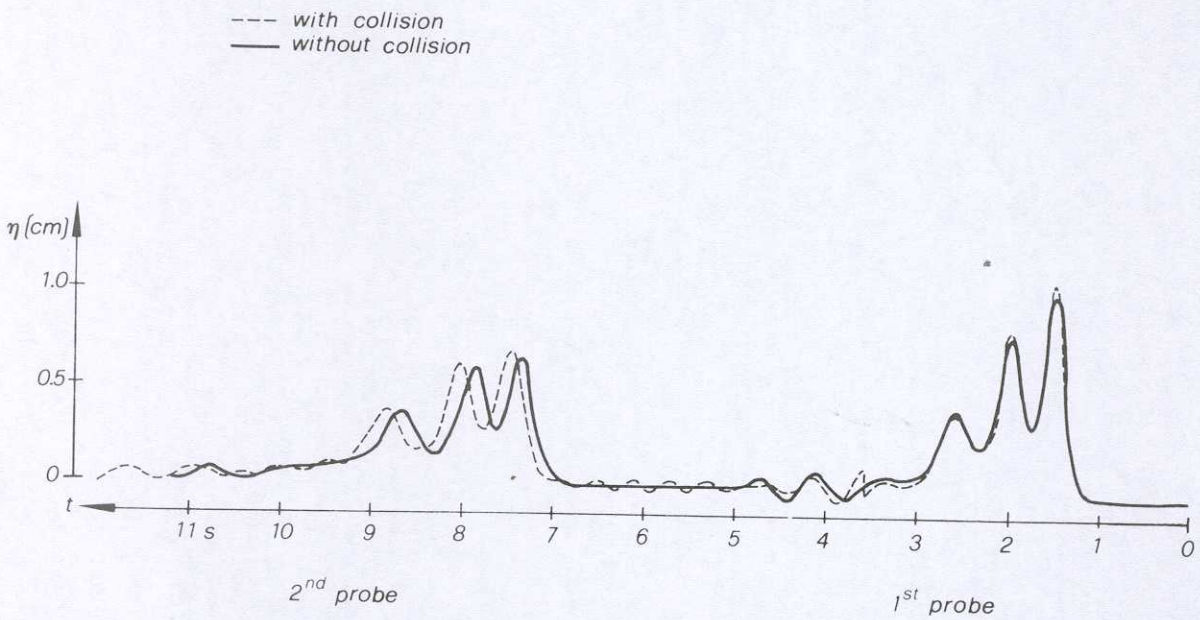

Fig. 10. The continuous curve is a record of a wave evolving into three solitons (initial conditions $A = 2$ cm, $B = 30$ cm, with $h = 4$ cm). The broken curve is a record of the wave evolving from identical initial condition but experiencing a collision with another group of solitons advancing in opposite direction between the two probes. Note that the phase delay in the presence of a collision is larger for smaller solitons.

group was generated with $A = 2$ cm, $B = 30$ cm; the colliding group was generated with $A = 2$ cm, $B = 20$ cm; the water depth was $h = 4$ cm and the probes were at $d_1 = 4$ m, $d_2 = 8$ m from the beginning of the tank. Separate observation of the colliding wave showed that it contained two solitons. The stability of the shape is immediately evident.

To have a more precise result a record was taken of the wave evolved by launching only the observed solition (i.e., without collision). The resulting curve is shown dashed in Fig. 10 superimposed in time over the previously discussed one at the first probe. At the second probe we observe three solitons in both cases; the shape of the corresponding solitons are identical. The only observed effect of the collision is a delay that is a decreasing function of the amplitude. Unfortunately the KdV equation does not give any prediction.

V. CONCLUSIONS

The wave tank we have described can be easily built in an average mechanical workshop, and be located in a students' laboratory.

As we have shown, the principal predictions of the KdV equation and more generally the behavior of nonlinear waves in water can be tested and observed by the students.

More experiments than those presented here are of course possible with the described apparatus (for example, observations of waves evolving from different initial shapes, of waves at the interface between two liquids, etc.).

In our laboratory the students are asked to define their own "research program" after a study of the relevant literature; they must also design, build, and test the detector to be used in the experiments. We have found that the students enjoyed working in the laboratory; some have been even motivated to continue the study of nonlinear waves in their thesis work. We believe the observed intellectual motivation originates from the possibility of choosing among different alternatives and the variety of arguments to be learnt, ranging from practical electronics to theoretical physics.

ACKNOWLEDGMENTS

The experiments described here have been possible due to the work of F. Fassò and G. Torzo who contributed to the design and testing phases and of B. Dainese and G. Veronese (INFN) who built and assembled the wave tank.

[1] N. J. Zabusky and M. D. Kruskal, Phys. Rev. Lett. **15**, 240 (1965).

[2] J. Scott Russell, "Report on Waves," in 1844 British Assn. Adv. Sci. Report (London, 1845) and in Proc. R. Soc. Edinburgh, 1844, p. 319.

[3] D. J. Korteweg and G. deVries, Philos. Mag. **39**, 422 (1895).

[4] See, for example: G. B. Whitman, *Linear and Nonlinear Waves* (Wiley, New York, 1974); G. A. Toomb, Eur. J. Phys. **1**, 162 (1980); H. Segur in *Topics in Ocean Physics*, Proc. Int. School E. Fermi, Course LXXX (North-Holland, Amsterdam, 1982); see also the contributions of J. Hammack and A. R. Osborne and T. L. Burch in the same Proceedings.

[5] As mentioned in the text we have neglected surface tension effects. This is justified if h is much bigger than a typical value h_T, that for water has the value $h_T = 0.48$ cm. Surface tension in fact modifies the dispersion relation; in Eq. (2) the factor $-(h^2/6)$ in front of the cubic term k^3 must be substituted by $-(h^2/6)[1-(h_T/h)^2]$, where $h_T = 3T/\rho g = 0.48$ cm for water at normal temperature (T is the surface tension). The effect of surface tension is to reduce the absolute value of the cubic term (that goes to zero at $h = h_T$). In our experiments we will work with depth values of 6 cm, 4 cm, and 3 cm, where the neglected correction term is 0.6%, 1.4%, and 2.6%, respectively.

[6] C. S. Gardner, J. M. Green, M. D. Kruskal, and R. M. Miura, Phys. Rev. Lett. **19**, 1095 (1967).

[7] H. Segur, J. Fluid Mech. **59**, 721 (1973).

[8] J. Hammack and H. Segur, J. Fluid Mech. **65**, 289 (1974).

[9] To be precise this is true only for instantaneous extraction. We have verified that the evolving solitary waves do not depend on the extraction time.

[10] A. Marchesin, F. Patarino, and P. Riello, class 1981–82.

Holographic detection of defects under the surface of solid objects[a)]

Thomas K. Hemmick, Jacob W. Huang, and Yu Dong Song[b)]

Department of Physics, Towson State University, Towson, Maryland 21204

(Received 14 January 1983; accepted for publication 10 February 1983)

In this paper we introduce a simple, low-cost experimental system designed to demonstrate the effectiveness and sensitivity of optical testing to undergraduate students. The technique used involves generating stress by heating a material locally and detecting by holographic interferometry.

I. INTRODUCTION

In 1965, double-exposure and real-time holographic interferometry techniques were developed independently by researchers in several laboratories. This includes the work of Horman,[1] Burch,[2] Powell and Stetson,[3–6] and Haines and Hildebrand,[7] who, among others[8–10] studied the surface deformation and displacement of diffusely reflecting objects. In more recent years researchers have worked with holographic techniques in production.[11]

We feel that experiments in optical testing should be performed on the undergraduate level. In this paper we introduce a simple undergraduate experiment whose results can be used to qualitatively identify material defects not visible